Spinodal decomposition of two-dimensional fluid mixtures: A spectral analysis of droplet growth

H. Furukawa

Faculty of Education, Yamaguchi University, Yamaguchi 753-8513, Japan

The spinodal decomposition of two-dimensional fluid mixture is studied by numerical simulation. For the high viscous fluid mixture it has not been evident whether the interfacial tension is relevant to the droplet growth or not. A length scale R defined by the structure function extracting the effect of the long wavelength mode justifies a rapid growth close to $R \sim t$, but the length scale energetically defined reveals a much slower growth $R \sim t^{0.5}$, where t is time. This discrepancy represents the violation of the dynamical scaling with single length scale. The slow gowth of the length scale is attributed to the accumulation of the number of isolated droplets in phase separating state, whereas the rapid growth represents the relevance of the surface tension as the driving force in two dimensions. For a low viscous fluid mixture the dynamical scaling is a good assumption with the growth law $R \sim t^{2/3}$ up to a very large Reynolds number Re$\sim$1500, which is the limit in the present simulation.

I. INTRODUCTION

When a fluid mixture is suddenly quenched into a thermodynamically unstable state the phase separation takes place (see Ref. [1] for reviews). If properties of two phases are nearly symmetric, the two phases mutually interconnect. Then Siggia [2] found that the interfacial tension is a relevant driving force for the droplet growth. The pressure difference originating from the interfacial tension and irregular interfacial shape induces convective fluid motions. Such motions accelerate the droplet growth. Based on the dynamical scaling hypothesis Siggia obtained a linear growth law of droplet $R \sim t$ for a viscous fluid mixture, where R and t are, respectively, the length scale and the time elapsing after the quench. The present author then pointed out that the Reynolds number Re increases indefinitely as time proceeds [3,4]. Therefore, the dissipation becomes irrelevant as the friction to the fluid motion in a long time limit, and a relevant friction to the fluid motion must be the inertia which decelerates the fluid motion [5]. We then obtain the growth law $R \sim t^{2/3}$ in the case of high Reynolds number [3]. Even in this case the dissipation is still needed for droplets to grow irreversibly [6].

The Reynolds number is defined by

$$\text{Re} = \frac{\text{inertial term}}{\text{dissipation term}} \sim \rho \eta^{-1} R U. \qquad (1)$$

Here U is a velocity of fluid in a scale length R, and ρ and η are mass density and shear viscosity, respectively. The crossover from $R \sim t$ to $R \sim t^{2/3}$ must occur at Re=1. However, if η/ρ is very large, we have a regime of small Re with large R. Such a regime actually exists, for instance, for polymer blends, and is treated as an actual late stage of the phase separation. We extract such a high viscosity state by setting the mass density zero or the viscosity infinity as usual, but we do not discuss a crossover between the high viscosity state and the low viscosity state.

Throughout this paper, for the sake of simplicity, we often do not represent physical quantities such as the shear viscosity η, the mass density ρ and the interfacial tension σ, in the growth law. Explicitly the above two growth laws are, respectively, written as $R \sim (\sigma/\eta)t$ and $R \sim (\sigma/\rho)^{1/3}t^{2/3}$.

These growth laws in some cases are examined numerically and experimentally, but the two-dimensional case is still under controversy. One of sources of the controversy is the growth mechanism of the high viscous fluid mixture. The linear growth law $R \sim t$ is explained by the interfacial tension and the energy dissipation which play roles respectively of a driving force and a friction to the fluid motion. There is an idea that the interfacial tension is irrelevant in two dimensions, and the growth law $R \sim t$ does not hold in two dimensions [7]. In fact there is no clear evidence for the observation of the linear growth law in two dimensions, but nonlinear growth laws seem to be suitable even for the symmetric quench of high viscous fluid mixtures in two dimensions [8]. It is, however, to be noted that we cannot conclude that the interfacial tension is not relevant in two dimensions, since other systems reveal clear evidence for the relevance of the interfacial tension in two dimensions. That is, the late stage of the coarsening process in nonhydrodynamic systems is governed by the growth law $R \sim t^{1/3}$ for conserved order parameter [9] and by $R \sim t^{1/2}$ for nonconserved order parameter [10]. These growth laws are nothing but originating from the interfacial tension. Furthermore the low viscous fluid mixture in two dimensions is known to exhibit a growth law $R \sim t^{2/3}$ [11] for which the interfacial tension is the driving force and the inertia act as the friction to the fluid motion. This is also evidence for the relevance of the interfacial tension in two dimensions.

The second controversy is about the limit of the Reynolds number in the coarsening process. Let the length scale R grows as t^a. Then the Reynolds number grows as Re $\sim t^{2a-1}$ [3]. Therefore, Re increases indefinitely, if $a > 1/2$. Recently, Grant and Elder [12] presented a doubt to the indefinite increase in the Reynolds number. They considered that the Reynolds number would not exceed a value about 10 or 100, so that the final value of the growth exponent a may not exceed 1/2 even in low viscous fluid mixture. The state of a high Reynolds number is turbulent. Grant and Elder considered that in a turbulent state the grown droplets would

be destroyed into pieces yielding many isolated spherical droplets just like stirred salad dressing [13]. On the contrary to this suspicion a preceding numerical simulation by the lattice Boltzmann gas [14] revealed an opposite feature of the phase-separating domain morphologies. Namely, many isolated spherical droplets are created not in the low viscous fluid mixture but in the high viscous fluid mixtures, exhibiting a break-down of the dynamical scaling [15]. On the contrary, the low viscous fluid mixture keeps a mutually interconnected domain structure. Therefore, the understanding of the coarsening mechanism of two-dimensional fluid mixture is not satisfactory, yet.

In this paper we present a numerical simulation of phase separation of two-dimensional low and high viscous fluid mixtures, in order to examine above mentioned problems using variously defined length scales. We then obtain the following conclusions, which are more quantitative than in previous numerical simulations. (1) Even for the high viscous fluid mixture the curvature driven growth law $R \sim t$ seems to gorvern the growth of larger droplets. (2) A seemingly delayed domain growth can be explained by considering an accumulation of number of isolated droplets and the violation of dynamical scaling with single length scale. (3) For a low viscous fluid mixture the length scale grows as $R \sim t^{2/3}$ up to extremely large Reynolds number larger than about 1500, which is the limit of the ability of the present numerical simulation. In the next section the model will be presented. Length scales are defined in several ways. In Sec. III numerical results are given and analyzed. In Sec. IV concluding remarks are presented.

II. MODEL AND PRELIMINARIES

We use the following model, which is a kind of so-called model H [16]:

$$\frac{\partial \psi}{\partial t} = -\boldsymbol{\nabla} \cdot \mathbf{v}\psi + \nabla^2 \mu, \tag{2}$$

$$\frac{\partial \phi}{\partial t} = -\boldsymbol{\nabla} \cdot \mathbf{v}\phi, \tag{3}$$

$$\rho \frac{\partial \mathbf{v}}{\partial t} = -\rho(\mathbf{v} \cdot \boldsymbol{\nabla})\mathbf{v} + \eta\nabla^2\mathbf{v} - \phi\boldsymbol{\nabla}\mu_\phi - \psi\boldsymbol{\nabla}\mu, \tag{4}$$

where ψ is the order parameter which takes the value 1 or -1 in equilibrium, ϕ is the total material density (number density), $\mathbf{v}$ is the velocity field of fluid, ρ is the mass density, and η is the shear viscosity. μ and μ_ϕ are the chemical potentials and are given by functional derivatives of the free energy F. The basic form of the chemical potentials are given by

$$\mu = \frac{\delta F}{\delta \psi} = -\frac{1}{2}\nabla^2\psi - (1-\psi^2)\psi, \tag{5}$$

$$\mu_\phi = \frac{\delta F}{\delta \phi} = \chi_0^{-1}(\phi - \phi_0), \tag{6}$$

where χ_0 is the compressibility and is chosen so that the system may be kept to be incompressible. Equation (5) can be amplified if necessary as

$$\mu \to \sigma^*\mu. \tag{7}$$

This makes the interfacial tension σ change into

$$\sigma \to \sigma^*\sigma, \tag{8}$$

since the change in the interfacial tension simply corresponds to the change in the energy scale. The positive constant σ^* is a reduced interfacial tension.

The above set of equations are solved numerically under a suitably random initial condition in discrete space of size 1024×1024. Two different cases are studied. One is a very viscous case, where we neglect both the left hand side and the first term on the right hand side of Eq. (4). The other is a very low viscous case, where we set $\eta = 0.01$. The estimated final Reynolds number is more than 1500.

We calculated variously defined length scales R's. Here, we shall mention them.

The free energy density f associated to the order parameter ψ is written as $f = f_K + f_P$, where

$$f_K \equiv \frac{1}{4}|\boldsymbol{\nabla}\psi|^2, \tag{9}$$

$$f_P \equiv \frac{1}{4}(1-\psi^2)^2. \tag{10}$$

f_K and f_P are analogous to the kinetic energy and the potential energy of the mechanics, respectively. It can be shown that the average of two densities are equal to each other if the interfaces of domains are clearly formed and the system becomes locally in equilibrium state (see Appendix A):

$$f_K(t) \sim f_P(t). \tag{11}$$

If the system is in a local equilibrium state, Eqs. (9) and (10) have nonvanishing value only at interfacial regions and, as a rule, are proportional to the average interfacial size per unit volume A:

$$\langle f_K(t) \rangle \sim A, \tag{12}$$

$$\langle f_P(t) \rangle \sim A. \tag{13}$$

Geometrically A can be given by directly measuring the length of the interfaces of domains, i.e., by counting lattice points of the discrete space where $\psi(\mathbf{r})\psi(\mathbf{r}') < 0$. Here $\mathbf{r}$ and $\mathbf{r}'$ indicate nearest-neighboring lattice points. For a single droplet with a radius R, we find that

$$A \sim \frac{R^{d-1}}{R^d} \sim R^{-1}. \tag{14}$$

Here d is the spatial dimensionality. If the dynamical scaling holds, A^{-1} is the length scale of the system just as Eq. (14).

We calculate energies $\langle f_K \rangle$ and $\langle f_P \rangle$, and the average interfacial size A, independently. Then, we relate these quantities to respective length scales R's:

$$R \sim \langle f_K(t) \rangle^{-1}, \tag{15}$$

$$R \sim \langle f_P(t) \rangle^{-1}, \tag{16}$$

$$R \sim A^{-1}. \tag{17}$$

These different length scales becomes equivalent to each other if the system is in a local equilibrium state. Therefore, the local equilibrium state of the system (the late stage of the phase separation) can be justified by comparing these three different length scales with each other.

The other method of evaluating the length scale is to use the structure function:

$$R = \left(\frac{\int S_k(t)k^m dk}{\int S_k(t)dk} \right)^{-1/m}, \tag{18}$$

where $S_k(t)$ is the structure function

$$S_k(t) = \langle |\psi_{\mathbf{k}}(t)|^2 \rangle, \tag{19}$$

and $\psi_k(t)$ the fourier component of the order parameter ψ. The structure function may have asymptotic forms

$$S_k(t) \sim k^\theta \quad (k \to 0), \tag{20}$$

$$S_k(t) \sim k^{-d-1} \quad (k \to \infty), \tag{21}$$

where $\theta = 4$ for solid and $\theta = 2$ for fluid [17]. Therefore, appropriate values of the power m may be $1 - \theta < m < d + 1$. However, we have extended the range of m by introducing a cutoff parameter for the k integration in Eq. (18). The length scale defined by Eq. (18) should not depend on the value m if the dynamical scaling holds: $S_k(t) = R(t)^2 \tilde{S}[kR(t)]$. That is, all length scales defined by Eqs. (15)–(18) should be the same if the dynamical scaling holds.

If the dynamical scaling does not hold, then the length scale defined by Eq. (18) does not coincide with others, because such a definition as Eq. (18) gives the m dependence on R: The behavior of modes with smaller wave number is characterized by smaller $m < 0$, whereas that with larger wave number is characterized by larger $m > 0$. Thus this provides with a kind of a spectral analysis of growth exponent a ($R \sim t^a$).

III. NUMERICAL RESULTS

A. High viscous case

We numerically solved Eqs. (2)–(6) in the limit of zero Reynolds number (Re=0). This case corresponds to setting $\rho = 0$. By neglecting the inertial terms in Eq. (4) we have

$$\eta \nabla^2 \mathbf{v} = \phi \mathbf{\nabla} \mu_\phi + \psi \mathbf{\nabla} \mu. \tag{22}$$

This equation is solved for $\mathbf{v}$ using the fast Fourier transform [18]. The velocity $\mathbf{v}$ thus solved is substituted into Eqs. (2) and (3). We reduced the amplitude of the chemical potential μ and the interfacial tension σ by setting $\sigma^* = 1/4$ [see Eqs. (7) and (8)]. We used discrete space of size 1024×1024, and then four different runs are averaged. We used a simple Euler method to solve the discretized equation. The discrete time Δt is $0.02 \leqslant \Delta t \leqslant 0.05$. Numerical results are insensitive to the value of Δt.
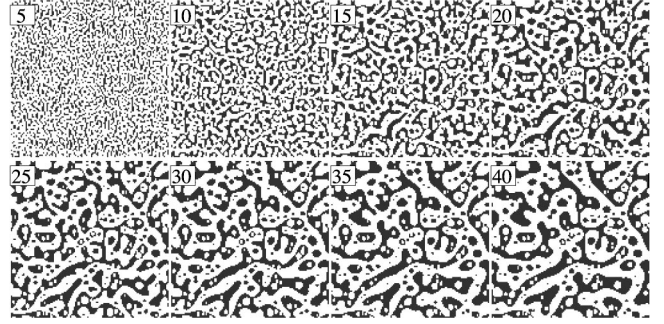

FIG. 1. Phase separation patterns in case of high viscosity, where the Reynolds number is set zero. The system size is 1024×1024, but only 128^2 points are displayed. The simulation time of each pattern is $100n$, with n being the number shown on the pattern.

We observed the same nonscaling morphology (see Fig. 1) as those of previous simulations [14,15]. In Fig. 2 three different length scales by Eqs. (15), (16), and (17) are compared. Each length scale is scaled by its own final value. We find that these three length scales nicely coincide with each other. Notice that such a coincidence does not guarantee the validity of the dynamical scaling but only means that the system is in a local equilibrium state. The most striking feature found from Fig. 2 is that the length scale R thus defined exhibits a small growth exponent near 1/2. We cannot find any evidence for the validity of the curvature (or interfacial tension) driven and dissipation controlled droplet growth law $R \sim t$. However, we cannot conclude that the curvature driven droplet growth is absent in two-dimensional viscous fluid mixture, since the dynamical scaling with a single length scale is violated in this case.

In Fig. 3 we present the length scale defined by Eq. (18) as a function of t for several values of m. In Fig. 4 the growth
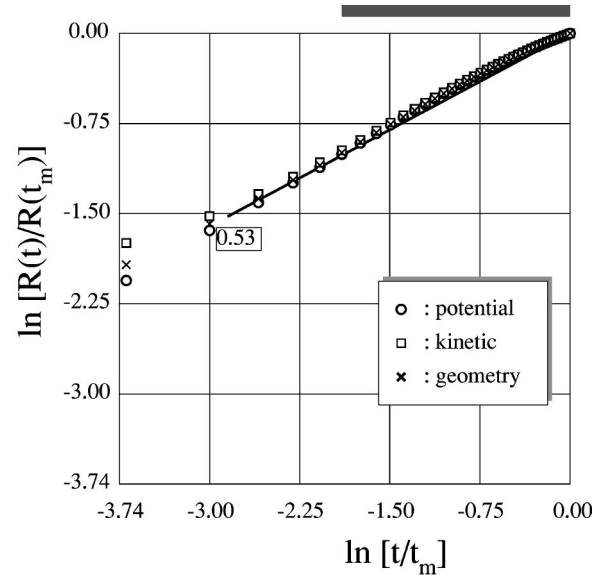

FIG. 2. Time dependences of length scales (15)–(17) in case of high viscosity. Kinetic, potential, and geometry indicate, respectively, Eqs. (15), (16), and (17). The slope of a straight line is given by the least square method using the data points in the range marked by a gray fat line. A weight function inversely proportional to the density of data points is used.
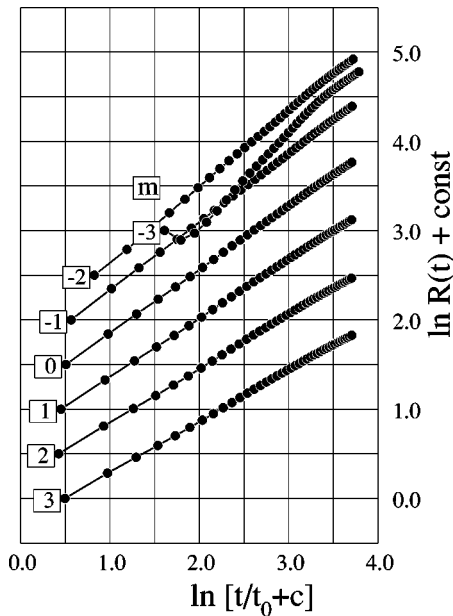
FIG. 3. Time dependence of length scale (18) in the case of high viscosity for several values of power m. Time is slightly shifted, $t/t_0 \rightarrow t/t_0 + c$, where t_0 is the first time of the output of data. The shift parameter c and the growth exponent a are determined by the least square method. A weight function inversely proportional to the density of data points is used. Each length scale at time t is given by Eq. (18) where the summation over k is cut off at $k = 5k_{\max}$. Here $k_{\max}$ is the peak position of the structure function.

exponents are shown as a function of m. To calculate the length scale using Eq. (18) we used a cutoff for the k integration. The cutoff is $k_c = 5k_{\max}$ with $k_{\max}$ being the wave number at which $S_k(t)$ has a peak. In Fig. 4 we compared two cases with the cutoff and without the cutoff. For large positive values of m these two cases give different results from each other. This is because S_k at large k is amplified for large m and dominates the integration. But for a discrete model, the amplification of small scale structure is meaningless. This is the reason why we introduced a cutoff. The length scale R seems to have the rapid growth component
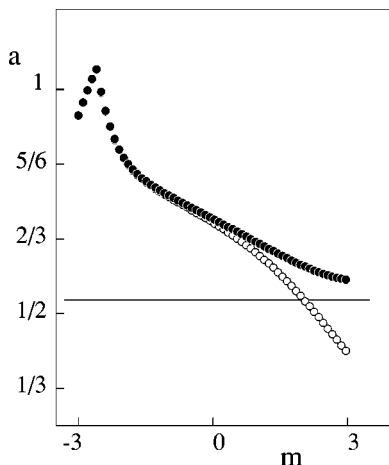

FIG. 4. The growth exponent a, corresponding to Fig. 3 as a function of m. For closed circles the summation over k in Eq. (18) is cut off at $k = 5k_{\max}$, whereas for open circles no cutoff is used. The horizontal line indicates the growth exponent value of Fig. 2.
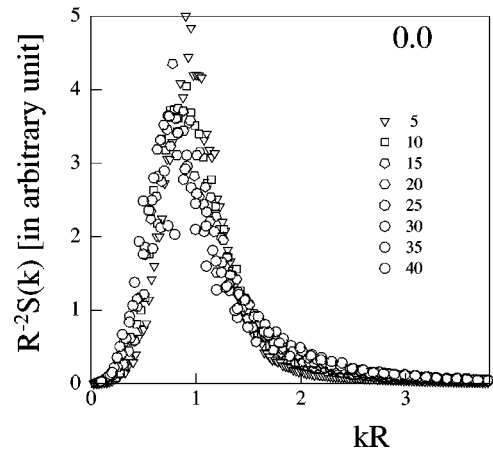

FIG. 5. Scaling plot of the structure function $S(k)$ in case of high viscosity. The length scale R is defined by Eq. (18) with $m \approx 0$. The symbols indicates data at times t's of the same unit as Fig. 1.

$R \sim t$. Such a rapid growth cannot be detected by other length scales. The strong m dependence of the growth exponent a, varying from about 0.5 to about 1, shows the violation of the dynamical scaling with single length scale. In Fig. 5 we show the scaling plot of the structure function: $R^{-2}S(k)$ as a function of kR. Here the length scale is defined by Eq. (18) with $m = 0$. Even except near the peak position where the fluctuation is intrinsically large, the scaling assumption seems to be poorly satisfied.

Here we consider the reason why two types of length scale exhibit very different growth behaviors. Due to the poor connectivity in two dimensions, isolated droplets are created in the process of the phase separation. In a viscous fluid an isolated droplet rapidly loses its kinetic energy and then comoves with an outer large droplet which is driven by the interfacial tension (see Fig. 1). Therefore, once an isolated droplet is created such a droplet lives for a long time. Therefore, the number of isolated droplets created at various times accumulates. We presented a primitive idea that such an accumulation may lead to an intermittent droplet growth changing the growth exponent [19].

Although it is difficult to explain quantitatively the modification of the growth exponent we can understand the reason why the modification of the growth exponent occurs by the accumulation of the isolated droplets. Let the length scale of largest droplets be R_O. It is assumed that largest droplets are interconnected. Therefore, the R_O can be assumed to grow fast as $\sim t$. The successive accumulation of the number of isolated droplets gives rise to a non-self-similar droplet morphology. The lower bound of the length scale R_o is the average size of initially created isolated droplets, which grows as $\sim t^a$ with $a = 1/2$ if the thermal fluctuation is effective. If the thermal fluctuation is not effective, then a is smaller than that. Let us consider a simple geometric length scale (17). The total interfacial size should be larger than R_O^{d-1} because of the successive accumulation of isolated droplets. Let the total size of the interface be R_O^{D-1}, with $d < D < d+1$. The interfacial size per unit volume is given by $R_O^{D-1}/R_O^d = R_O^{-I}$, where $I = d + 1 - D$. For example, if $D = d + 1/2$, then we have $I = 1/2$. We then observe $R_O^{1/2} (= R_O^I)$ as the simple geometric length scale (17). Therefore, even if the largest
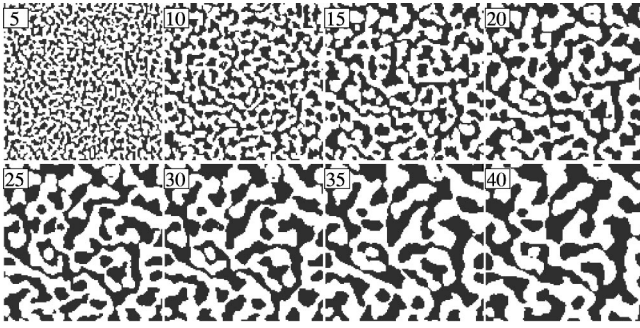
FIG. 6. Phase separation patterns in case of low viscosity. The system size is 1024×1024, but only 128^2 points are displayed. The simulation time of each pattern is $50n$, with n being the number shown on the pattern.

droplets grow rapidly as $R_O\sim t$, the simple geometric length scale defined by Eq. (17) behaves as $R\sim t^{1/2}$ ($=t^l$).

The accumulation of isolated droplets would occur more hardly in three dimensions than in two dimensions, because of a rich connectivity among droplets in three dimensions. Therefore the dynamical scaling with single length scale may be more appropriate for the three dimensional viscous fluid mixture [20].

B. Low viscous case

For a low viscous case, we set $\rho=1$ and $\eta=\nu=0.01$. The reduced interfacial tension is set as $\sigma^*=1$. We numerically solved Eqs. (2)–(6) in discrete space-time of a size 1024×1024, and then four different runs are averaged. We used a simple Euler method to solve discretized equations. The discrete time interval Δt is $0.0125\leqslant\Delta t\leqslant0.025$. Numerical results are insensitive to the value of Δt. The same analyses as those for the high viscous case are shown in Figs. 6–8. In Fig. 6 the coarsening patterns are shown. In Fig. 7 the time-dependences of length scales defined by Eqs. (15)–(17) are shown. Three length scales are scaled by their own final values. The growths of these length scales are charac-
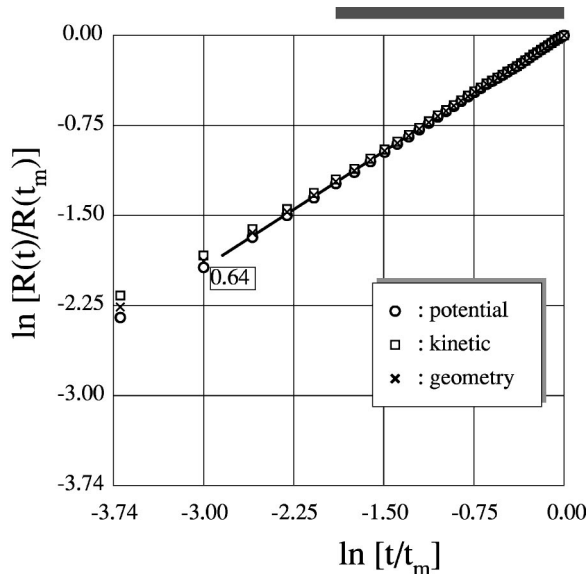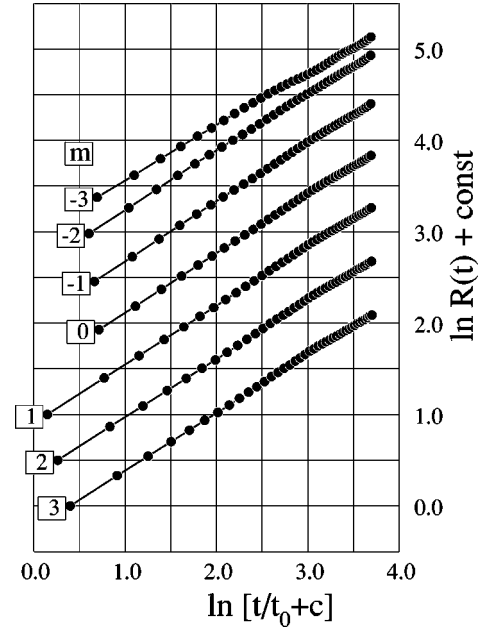

FIG. 8. Time dependence of length scale (18) in case of low viscosity (see the caption of Fig. 3 for the explanation).

terized by a single growth law $R\sim t^{2/3}$ as expected. It is also found that the system is in a local equilibrium state. In Fig. 8 the length scale defined by using the structure function (18), is shown for several values of m as functions of t. In Fig. 9 the growth exponent thus obtained is shown as a function of m. It can be found that the growth of the length scale hardly depends on m. This means that the scaling holds in low viscous case. The growth exponent in Fig. 9 coincides with that in Fig. 7: all length scales obey the same growth law $R\sim t^{2/3}$. In Fig. 10 we show the scaling plot of the structure function: $R^{-2}S(k,t)$ as a function of kR. Here the length scale is defined by Eq. (18) with $m\approx0$. The scaling assumption seems to be better satisfied than the high viscosity case of Fig. 5.

We evaluated the final value of the Reynolds number Re (1). Here $\rho=1$ and $\eta=0.01$ in the present simulation. U is an instantaneous velocity of fluid, which may not be smaller

FIG. 7. Time dependences of length scales (15)–(17) in case of low viscosity (see the caption of Fig. 2 for the explanation).
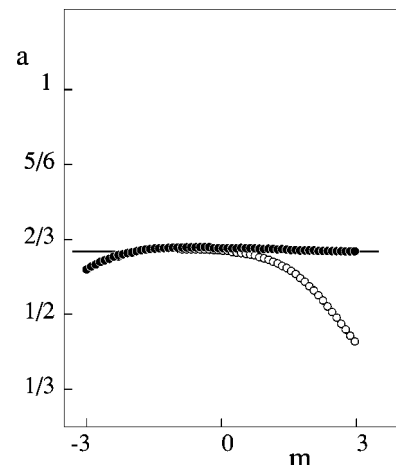

FIG. 9. The growth exponent a, corresponding to Fig. 8 as a function of m (see the caption of Fig. 4 for the explanation). The horizontal line indicates the growth exponent value of Fig. 7.
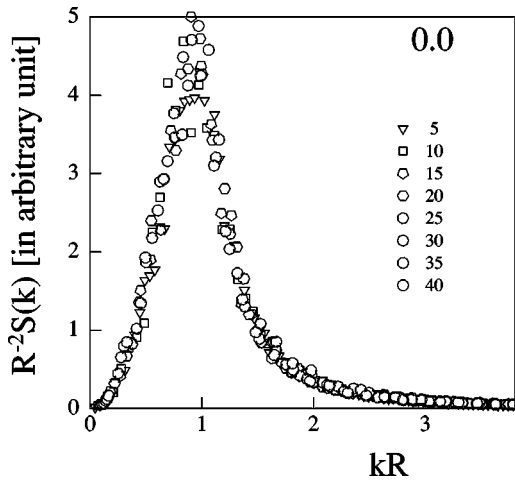
FIG. 10. Scaling plot of the structure function $S(k)$ in case of low viscosity. The symbols indicates data at times t's of the same unit as Fig. 6.

than $dR(t)/dt \sim R/t$, because dR/dt is not a true velocity of fluid, but averaged one. Therefore, we may have

$$\mathrm{Re} > \frac{R^2}{\nu t}. \tag{23}$$

In our simulation the size of a cell of the discretized space is set to be 1, and the $\nabla^2 \mathbf{v}$ is calculated simply as

$$\nabla^2 \mathbf{v} \rightarrow \mathbf{v}(x+1,y) + \mathbf{v}(x-1,y) + \mathbf{v}(x,y+1) + \mathbf{v}(x,y-1)$$
$$-4\mathbf{v}(x,y),$$

where x and y indicate positions in the discrete space. The unit of time is 1. The maximum computation time is 2000 and the final average droplet size is about 170. By substituting approximate values $\nu t \sim 20$ and $R \sim 170$, we find that the final Reynolds number calculated by Eq. (23) is

$$\mathrm{Re} \sim 1500. \tag{24}$$

This value is about 15 times larger than the critical value predicted by Grant and Elder [12].

Grant and Elder criticized that the discretized model may not give a correct value of the Reynolds number. They suggested that the minimum spatial length scale, i.e., the lattice spacing, should be relevant to the Reynolds number. However, it was not evident how the microscopic scale is relevant to the evaluation of the macroscopic Reynolds number. Here we shall show that the microscopic length scale is not relevant to the evaluation of the Reynolds number if we use a suitable phenomenological model. This can be done by finding out how microscopic scales comes out in the phenomenological model. In the phenomenological hydrodynamic equation (4) a microscopic quantity η is treated as a parameter. As is well known in standard statistical mechanics, such a parameter, which puts implicit microscopic space-time scales into the model, is produced by averaging out the microscopic degrees of freedom of the mechanical equation. Therefore, concerning to the phenomenological equation, no fine space-time region for averaged-out microscopic motion is necessary and any macroscopic motion is free from such

microscopic scales. As an example, consider a linearized hydrodynamic equation and assume to make a suitable coarse graining in space. It is evident that a coarse-grained cell size is not relevant to the fluid motion with a length scale larger than the coarse-grained length (this means that the Reynolds number should be independent of the coarse-grained cell size). Since the Reynolds number $\mathrm{Re} \sim R^2/(\nu t)$ contains a microscopic quantity $\nu \equiv \eta/\rho$, it may exhibit small scales. For the present simulation we have $\mathrm{Re} \sim (R/r_0)^{1/2}$ using $R \sim t^{2/3}$. Here r_0 is a constant representing a length scale, and takes a very small value $\sim 10^{-4}$ in the late stage of the present simulation. This must be a source of the criticism by Grant and Elder. But such a small length scale should not be attributed to the discreteness of the macroscopic model. It is more important to find out whether macroscopic fluid motions are closed within the discrete model or not. If motions are closed within the discrete model, then the Reynolds number can be safely evaluated by Eqs. (1) or (23). For this purpose we shall examine the length scale where the energy is dissipated and the corresponding fluid motion is frozen in.

We first consider the energy dissipation under an extreme condition. We assume that the kinetic energy supplied from the surface tension at the length scale R is dissipated only at a small scale λ, where the dissipation would dominate the inertial motion. λ can be evaluated by balancing the energy dissipation with the energy supply from the surface tension. The supplied surface energy is $\sigma/(tR)$ per unit volume and unit time. The energy dissipation per unit volume per unit time is $0.5\eta|\nabla \mathbf{v}|^2 \sim \eta/\tau^2$. Here $\tau \sim \lambda^2/\nu$ is the characteristic time of the dissipative motion at the length scale λ. The balance between the energy supply and the energy dissipation gives $\sigma/(tR) \sim \eta/\tau^2$, which gives $\tau^2 \sim t\eta R/\sigma$ or $\lambda^4 \sim \rho \nu^3 Rt/\sigma$. Using the Reynolds number $\mathrm{Re} \sim R^2/(\nu t)$, and the growth law $R \sim (\sigma/\rho)^{1/3} t^{2/3}$, we find that

$$\lambda \sim \left(\frac{\rho}{\sigma}\right)^{3/8} \nu^{3/4} R^{5/8} \tag{25}$$

$$\sim (\mathrm{Re})^{-3/4} R. \tag{26}$$

In the final stage of the present simulation we have $\lambda \sim 0.7$. This value is somewhat smaller than the lattice spacing 1. If the minimum length scale is relevant to the evaluation of the Reynolds number, Eq. (26) should give $\mathrm{Re} \lesssim R^{4/3}$ ($\lambda \gtrsim 1$). Even under this restriction we have a Reynolds number $\mathrm{Re} \sim 1000$ in the final stage of the simulation, which is still large. If we use larger kinetic viscosity $\nu = 0.1$, the final Reynolds number is about 150, and the length scale $\lambda \sim 4$. Even in this case the coarsening process is almost the same as that for $\nu = 0.01$, in the inertial range ($\mathrm{Re} > 1$). We therefore consider that the macroscopic behavior is hardly affected by the microscopic detailes of the model equation at least in the present simulation.

Equation (25) or (26) is an extreme case. Even in the inertial range ($\mathrm{Re} > 1$) the energy is dissipated. As a zeroth approximation the hydrodynamic equation can be written as $\rho d\mathbf{v}/dt \sim \mathbf{F}$, where $\mathbf{F}$ represents the last two terms on the right hand side of the hydrodynamic equation (4). Substituting the solution of this approximate equation, $\mathbf{v} \sim \mathbf{F}t/\rho$, into the second term on the right hand side of Eq. (4) we can evaluate the energy dissipation in the inertial range. This can

be conveniently done in the Fourier space. Let k_ℓ be the upper bound of the wave number of the energy dissipation. Then the energy dissipation can be evaluated as $\Sigma_{k<k_\ell}\eta k^2\langle|\mathbf{F}_k|^2\rangle t^2\rho^{-2}$. Since the force term $\mathbf{F}$ is not a conserved quantity and is of the order of $(\sigma/R)/R$, we find that $\langle|\mathbf{F}_k|^2\rangle\sim\langle|\mathbf{F}_0|^2\rangle\sim\sigma^2 R^{-2}$ $(=\sigma^2 R^{d-4})$. Then the energy dissipation in the inertial range is evaluated as $\eta(\sigma t k_\ell^2)^2/(\rho R)^2$ in two dimensions. By balancing thus evaluated energy dissipation with the energy supply $\sigma/(Rt)$ and using the relations $R\sim(\sigma/\rho)^{1/3}t^{2/3}$ and $\mathrm{Re}\sim R^2/(\nu t)$ we obtain [21]

$$\frac{1}{k_\ell}\sim\left(\frac{\rho}{\sigma}\right)^{1/8}\nu^{1/4}R^{7/8} \tag{27}$$

$$\sim(\mathrm{Re})^{-1/4}R. \tag{28}$$

In the final stage of the present simulation we obtain $k_\ell\sim1/30$. The corresponding value of the length scale is larger than the lattice spacing 1. It is also larger than λ, as expected.

From the above evaluations we may conclude that the energy dissipation is done in scales larger than or comparable to the lattice spacing at least in the late stage of the present simulation. Nevertheless, we did not observe any symptom of the break up of growing droplets nor the slowing down of the droplet growth. Grant and Elder [12] supposed that the droplet would break up into pieces at large Reynolds number for which the system becomes turbulent. This is true if the fluid is externally forced to a turbulent state [22]. However, in the present case the turbulence is self-induced due to the release of the interfacial energy. The present author once examined the stability of the droplet growth in such a self-induced turbulent state [6]. Following this examination droplets are not destroyed even by the turbulent motion, for two reasons. One reason is that the turbulent kinetic energy is not supplied externally as ordinary hydrodynamic turbulence is, but supplied by the reduction of the interfacial size [23]. Therefore, this energy is not large enough to redestroy droplets. The second reason is that the characteristic time of the energy dissipation in the turbulent state is of the same order as that of the droplet growth. Therefore, the kinetic energy of the turbulent motion is not accumulated during the growth of the droplet. If, however, droplet interfaces are deformed or if droplets are redestroyed due to the turbulent motion, then the growth law would be modified from $R\sim t^{2/3}$ to $R\sim t^{3/5}$ $[R\sim(\sigma\eta/\rho^2)^{1/5}t^{3/5}]$ [24]. But the growth law observed for the low viscous fluid mixture is not $t^{3/5}$ type but $t^{2/3}$ type. We examined this in the following way. If the droplet growth is not like $t^{2/3}$, then a dimensional analysis provides with another growth law with an arbitrary growth exponent a [24]:

$$R\sim\sigma^{2a-1}\rho^{a-1}\eta^{2-3a}t^a. \tag{29}$$

We define a reduced length scale R^*

$$R^*=\frac{R}{\sigma^{2a-1}\rho^{a-1}\eta^{2-3a}}. \tag{30}$$

R^* does not depend on σ, η, or ρ, if a correct exponent a is given. We compared two different runs changing the interfacial tension according to Eq. (7) or (8), i.e., one run for σ^*
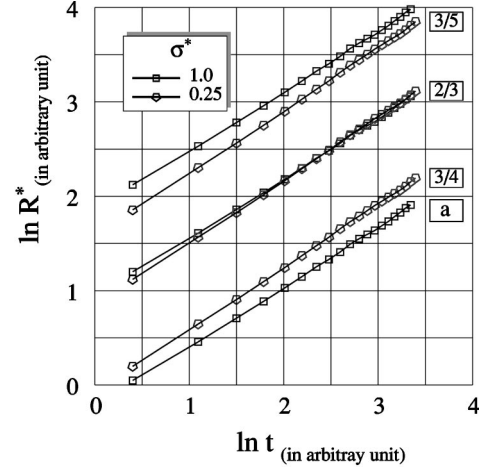

FIG. 11. Time dependences of reduced length scale R^* given by Eq. (30) in the case of low viscosity for two different interfacial tensions $\sigma^*=1$ and $1/4$ (in a reduced unit) for assumed three different growth exponent $a=3/5$, $2/3$, $3/4$.

$=0.25$ with $\eta=0.01$ and $\rho=1$, and compared it with the other run with $\sigma^*=1$ with $\eta=0.01$ and $\rho=1$. In Fig. 11 we compare reduced length scales R^* in two cases for three different growth exponents $a=3/5$, $2/3$, $3/4$ $(=0.6, 0.6667, 0.75)$. The range of time is the same as that of Figs. 6–8. We see that a reduced length scale R^* in two cases agrees with each other for $a=2/3$. Thus, the droplet growth we observed is $R\sim t^{2/3}$.

The reason why an isolated droplet is hardly formed in the turbulent state is as follows. In a turbulent state each droplet rapidly changes its position and shape. Therefore, even if an isolated droplet is formed, such a droplet soon touches on another droplet. Once a droplet touches on another one, they coalesce into a single droplet. On the contrary, for the high viscous fluid mixture, any isolated droplet loses its kinetic energy rapidly. Then, isolated droplets seldom meet. Therefore, an isolated droplet lives for a long time in a viscous fluid mixture.

IV. CONCLUDING REMARKS

We have numerically examined the dynamics of the late stage of the phase separation of fluid mixtures critically quenched, i.e., $\langle\psi\rangle=0$, in two dimensions. We considered two different cases, i.e., the high viscous and the low viscous fluid mixtures. The droplet growth is analyzed by means of variously defined length scales.

For a high viscous liquid mixture, the length scale defined by the structure function does not agree with other length scales which are defined by the energy and the interfacial size of droplets. In two dimensions, many isolated droplets are created during the phase separation [14] and such isolated droplets live for a long time because droplets lose their kinetic energies rapidly. Therefore, the number of isolated droplets of various sizes accumulates. This leads to the violation of dynamical scaling with single length scale and effectively reduces the droplet growth. However, the growth of the largest droplet is close to $R\sim t$, which originates from the interfacial tension. Such a rapid growth is reflected in the length scale defined by the structure function (18). This

means that the interfacial tension is relevant in two-dimensional high viscous fluid mixture.

For a low viscous fluid mixture we ascertained that the droplet grows as $R \sim t^{2/3}$ up to about a Reynolds number 1500. In contrast to the prediction by Grant and Elder [12], we cannot find any slowing down in the droplet growth or any destruction of grown droplets. This observation suggests an indefinite increase in the Reynolds number rather than the saturation. This feature may be explained by the two facts [6] that the time scale of the energy dissipation in a turbulent state is of the same order as the droplet growth and that the kinetic energy of turbulent fluid motion is originated from the reduction of the interfacial size. Therefore, the kinetic energy of turbulence is not sufficient to redestroy any grown droplet even at high Reynolds numbers. One recent numerical simulation shows that the low viscous droplet growth is stable even against the thermal noise [25]. Another recent numerical simulation in three dimsnsions up to the Reynolds number 350 supports the growth law $R \sim t^{2/3}$, but reveals no saturation of the Reynolds number [26]. At this moment, therefore, the saturation of the Reynolds number Re suggested by Grant and Elder has not been observed.

For the low viscous fluid mixture the dynamical scaling holds. This is because droplets have a kinetic energy sufficient for traveling. Thus an isolated droplet is soon caught by other droplet, and only small number of isolated droplets remain in a phase-separating low viscous fluid mixture.

When the Reynolds number increases indefinitely, the interfacial energy ϵ_1 and the hydrodynamic energy ϵ_2 per unit volume, and the Reynolds number behaves as $\epsilon_1 \sim \epsilon_2 \sim 1/R$, and $\mathrm{Re} \sim R^{1/2}$, respectively. The evaluation of ϵ_2 is due to the fact that the characteristic fluid velocity is given by $R/t \sim t^{-1/3} \sim R^{-1/2}$. The excess energy of the transient state is always two times larger than that of a corresponding thermal equilibrium state (Re$=0$ and $\epsilon_2=0$). In the inertial range the velocity field has the same characteristic time as that for a droplet to grow. Therefore, if a nonequilibrium state with a length scale R is assumed to be transformed into an equilibrium state (Re$=0$), it takes a time of the same order as that for a droplet to grow to a size R. In this sense the hydrodynamic transient state of an infinitely large system seems to approach a state different from the thermal equilibrium state.

APPENDIX A: LOCAL EQUILIBRIUM AND EQUIVALENCE OF KINETIC AND POTENTIAL PARTS OF FREE ENERGY

Let f be the free energy density: $f = f_K + f_P$, where f_K and f_P are given by Eqs. (9) and (10), respectively. A complete equilibrium state is represented by $\delta F/\delta \psi = 0$, where $F = \int f d\mathbf{r}$ is the total free energy of the system. This gives

$$-\frac{1}{2} \nabla^2 \psi + (\psi^2 - 1)\psi = 0. \qquad (A1)$$

In the late stage of the phase separation the system is not in a complete equilibrium state, but it may be in a local equilibrium state. We mean the local equilibrium state as a state where certain modes are in an equilibrium state but remaining modes are not in an equilibrium state. In the phase separation interfaces are clearly formed and the shapes of these interfaces change in time. Both the thickness of the interface and the composition of each phase can be assumed to be independent of time. Therefore, the profile of the interface is determined by the same equation as the equilibrium one. Let ℓ be a one-dimensional coordinate perpendicular to the domain interface. Then the order parameter should obey the following one-dimensional differential equation:

$$-\frac{1}{2} \frac{\partial^2 \psi}{\partial \ell^2} + (\psi^2 - 1)\psi = 0. \qquad (A2)$$

By multiplying this equation by $\partial \psi/\partial \ell$ and integrating by ℓ we obtain

$$\frac{1}{2}\left(\frac{\partial \psi}{\partial \ell}\right)^2 = \frac{1}{2}(1 - \psi^2)^2, \qquad (A3)$$

where we have used a boundary condition $\psi^2 = 1$ at $\ell = \pm\infty$. Since ℓ is perpendicular to the interface, we see

$$\mathbf{e}\partial \psi/\partial \ell = \nabla \psi, \quad (\partial \psi/\partial \ell)^2 = |\nabla \psi|^2, \qquad (A4)$$

at the interface, where $\mathbf{e}$ is a unit vector along the axis ℓ. ψ may be set constant outside the interfacial region. Therefore, we can assume that Eq. (A4) holds everywhere. Thus Eq. (A3) can be rewritten, using Eq. (A4), as

$$\frac{1}{4}|\nabla \psi|^2 = \frac{1}{4}(1 - \psi^2)^2 \qquad (A5)$$

or

$$f_K = f_P. \qquad (A6)$$

Notice that

$$\frac{\partial^2 \psi}{\partial \ell^2} \neq \nabla^2 \psi, \qquad (A7)$$

in general even if Eq. (A4) holds, since $\partial \mathbf{e}/\partial \ell \neq 0$. Therefore

$$\mu \equiv \frac{1}{2}\nabla^2 \psi + (\psi^2 - 1)\psi = \frac{1}{2}(\nabla^2 - \partial^2/\partial \ell^2)\psi \neq 0, \quad (A8)$$

in general. Here Eq. (A2) is used to derive the last side. Nonvanishing chemical potential (A8) gives a driving force of the phase separation.

---

[1] J.D. Gunton, M. San Miguel, and P.S. Sani, *Phase Transition and Critical Phenomena*, edited by C. Domb and J.L. Lebowitz (Academic, London, 1983), Vol. 8; H. Furukawa, Adv. Phys. **34**, 703 (1984); K. Binder, *Material Sciences and Technology*, edited by R. W. Cohen, P. Haasen, and E.J. Kramer (VCH, Weinheim, 1991), Vol. 5, p. 405; A.J. Bray, Adv. Phys. **43**, 357 (1994).

[2] E.D. Siggia, Phys. Rev. A **20**, 595 (1979).

[3] H. Furukawa, Phys. Rev. A **31**, 1103 (1985); Phys. Rev. E **55**, 1150 (1997).

[4] When the Reynolds number increases indefinitely, it seems that the final state, which may be an equilibrium state, is a peculiar state with an infinite Reynolds number. But this does not happen. If the system is finite, then such a peculiar state does not exist. If the system is infinite, then no equilibrium state is attained and therefore the Reynolds number increased indefinitely, though the characteristic velocity R/t goes to zero as $t^{-1/3}$, and any local part of the system would approach a local equilibrium state. However, no thermal equilibrium state with an infinite Reynolds number exists.

[5] If the friction is simply written in the same way as the inertia, then a difficulty arises. The inertia d^2R/dt^2, is negative in almost all cases, whereas the dissipative term, which is proportional to dR/dt, is positive. This is because $R \sim t^a$ and $a \leqslant 1$ in almost all cases. Therefore, the inertial friction should be proportional to $R/t^2 (>0)$. This form is natural if the dynamical scaling hypothesis is used.

[6] H. Furukawa, Phys. Rev. A **36**, 2288 (1987).

[7] M. San Miguel, M. Grant, and J.D. Gunton, Phys. Rev. A **31**, 1001 (1985).

[8] H.M. Tanaka, Prog. Theor. Phys. **100**, 1281 (1998).

[9] I.M. Lifshitz and V.V. Slyozov, J. Phys. Chem. Solids **19**, 35 (1961).

[10] S.M. Allen and J. W. Cahn, Acta Metall. **27**, 1085 (1979).

[11] See the second reference of Ref. [3], and references cited therein.

[12] M. Grant and K.R. Elder, Phys. Rev. Lett. **82**, 14 (1999).

[13] However, isolated domains in salad dressing may be rather due to asymmetric properties of two phases. For an example of such an asymmetric quench, see, A. Onuki and H. Nishimori, Phys. Rev. B **43**, 13 649 (1991).

[14] A.J. Wagner and J.M. Yeomans, Phys. Rev. Lett. **80**, 1429 (1998).

[15] A similar aspect was found by H. Tanaka and T. Araki, Phys. Rev. Lett. **81**, 389 (1998) in an early stage of the phase separation of fluid mixture.

[16] K. Kawasaki, Ann. Phys. (N.Y.) **61**, 1 (1970); B.I. Halperin, P.C. Hohenberg, and E.D. Siggia, Phys. Rev. Lett. **32**, 1289 (1974); J.E. Farrel and O.T. Valls, Phys. Rev. B **40**, 7027 (1989); **42**, 2353 (1990).

[17] The asymptotic form at large k is known as the Pord tail. G. Pord, Kolloid-Z. **123**, 83 (1951); **125**, 51 (1952); H. Tomita, Prog. Theor. Phys. **72**, 656 (1984); **75**, 482 (1986); for the asymptotic form at small k, see C. Yeung, Phys. Rev. Lett. **61**, 1135 (1988); H. Furukawa, *ibid.* **62**, 2567 (1989).

[18] Such a method is used by T. Koga and K. Kawasaki, Phys. Rev. A **44**, R817 (1991); Physica A **196**, 389 (1993).

[19] H. Furukawa, Prog. Theor. Phys. **71**, 438 (1984).

[20] The numerical test of the dynamical scaling for three-dimensional viscous fluid mixture seems to be in process. See S.I. Jury, P. Bladon, S. Krishna, and M.E. Cates, Phys. Rev. E **59**, R2535 (1999), and reference cited therein.

[21] This is already given by Eq. (A10) of the second citation of Ref. [3].

[22] A. Onuki, Phys. Rev. A **34**, 3528 (1986).

[23] The creations of an isolated droplet in viscous fluid mixture is due the weak connectivity in two dimensions. Such a creation of an isolated droplet occurs even in low viscous fluid mixture.

[24] See the second citation of Ref. [3].

[25] G. Gonnella, E. Orlandini, and J.M. Yeomans, Phys. Rev. E **59**, R4741 (1999).

[26] V.M. Kendon, J-C. Desplat, P. Bladon, and M.E. Cates, Phys. Rev. Lett. **83**, 576 (1999).